Distinct early transcriptional regulations by turgor and osmotic potential in the root of Arabidopsis

Amandine Crabos, Yunji Huang, Thomas Boursat, Christophe Maurel, Sandrine Ruffel, Gabriel Krouk, Yann Boursiac

Distinct early transcriptional regulations by turgor and osmotic potential in the root of Arabidopsis

Amandine Crabos*, Yunji Huang*, Thomas Boursat, Christophe Maurel, Sandrine Ruffel, Gabriel Krouk, Yann Boursiac

*: contributed equally to the work

Institute for Plant Sciences of Montpellier (IPSiM), Univ Montpellier, CNRS, INRAE, Institut Agro, Montpellier, France

TB is also affiliated to : Laboratoire de Mécanique et Génie Civil (LMGC), Univ Montpellier, CNRS, Montpellier, France

Amandine Crabos: amandine.crabos@inrae.fr 0000-0002-9746-4121

Yunji Huang: yunji.huang@supgaro.fr 0000-0001-8762-1560

Thomas Boursat: thomas.boursat@umontpellier.fr 0000-0001-6191-9289

Christophe Maurel: christophe.maurel@cnrs.fr 0000-0002-4255-6440

Sandrine Ruffel: sandrine.ruffel@inrae.fr 0000-0002-5651-8349

Gabriel Krouk: gabriel.krouk@cnrs.fr 0000-0003-3693-6735

Yann Boursiac: yann.boursiac@inrae.fr 0000-0002-9545-9003

Author for correspondence: Yann Boursiac, yann.boursiac@inrae.fr

Submission date :25/07/2023

Word counts (excluding M&M): 4507, number of tables: 1, number of figures: 6, number of supplemental data: 4

Short title: Turgor and osmotic potentials trigger distinct transcriptional responses

Highlight: Osmotic and turgor potentials shape specific transcriptional responses in the root of Arabidopsis under osmotic challenges.

Abstract

In a context of climate change, deciphering signaling pathways driving plant adaptation to drought, changes in water availability, and salt is key. A crossing point of these plant stresses is their impact on plant water potential (Ψ), a composite physico-chemical variable reflecting the availability of water for biological processes such as plant growth and stomatal aperture. The Ψ of plant cells is mainly driven by their turgor and osmotic pressures. Here we investigated the effect of a variety of osmotic treatments in the root of Arabidopsis plants grown in hydroponics. We used, among others, a permeating solute as a way to differentiate variations on turgor from variations in osmotic pressure. Measurement of cortical cell turgor pressure with a cell pressure probe allowed to monitor the intensity of the treatments and thereby preserve the cortex from plasmolysis. Transcriptome analyses at an early time point (15min) showed specific and quantitative transcriptomic responses to both osmotic and turgor pressure variations. Our results highlight how water-related biophysical parameters can shape the transcriptome of roots under stress and provide putative candidates to explore further the early perception of water stress in plants.

Keywords: ethylene glycol, NaCl, osmotic pressure, sorbitol, transcriptional response, turgor pressure, PEG, water potential

Abbreviations:

EG	Ethylene glycol
PEG	Poly ethylene glycol
P	Turgor pressure (MPa)
Π	Osmotic pressure (MPa)
Ψ	Water potential (MPa)
DEPs	Differentially expressed probes
DEGs	Differentially expressed genes

Introduction

How the environment is perceived by plants is of major importance for their life cycle. This is particularly true for water deficit (Maurel and Nacry, 2020; Verslues *et al.*, 2023) which can be summarized as an imbalance between the plant's requirement and loss of water and its uptake capacity. Water deficit directly impacts the plant water status. One of the ways plant water status is assessed is via plant water potential (Ψ), a composite variable which, in plant cells, integrates the turgor potential (or turgor pressure, P) and the osmotic potential (Π) (Haswell and Verslues, 2015). When considering the soil/plant/atmosphere continuum, Ψ can also be influenced by gravity and matric potentials. Ψ gradients allow evaluating the motive forces that generate net flows of water between different compartments of this continuum. Together with the viscoelastic properties of the cell wall, P is responsible for the elongation of cells and organs, and for the rigidity of stems and leaves, allowing them to act against gravity and optimize light interception, among others. Π is related to the concentration of solutes in a compartment. The presence of a Π gradient across a semi-permeable barrier causes osmosis: a net directional flow of water, even in the absence of any hydrostatic pressure difference (Bowler, 2017). Π influences biochemical reactions, and can be directly regulated by the cell through osmoticum accumulation, synthesis, and transport (Beauzamy *et al.*, 2014).

A critical issue in plant biology is to understand which physico-chemical parameters are perceived by plants. Terms such as osmosensing and mechanosensing are employed to describe phenomena related to perceiving the plant water status (Beauzamy *et al.*, 2014; Haswell and Verslues, 2015; Hamant and Haswell, 2017; Scharwies and Dinneny, 2019). Many molecular actors, such as mechanosensitive channels and protein kinases from multiple families (detailed in the reviews cited above) are thought to be involved in this perception or are contributing to associated phenomena. However, we lack a clear picture of the early perception of water deficit. One difficulty is that water deficit translates into multiple variations in the cell status. It is still discussed, for example, whether Π or P changes are directly sensed by plants or whether it is rather their impact on cell processes, cell wall status or cell volume (Sack *et al.*, 2018; Verslues *et al.*, 2023).

Another difficulty is that the links between the intensity of the stress causing the water deficit and cells parameters is hard to establish. Measuring plant physico-chemical parameters under physiological conditions is indeed difficult at cell-scale resolution. Π or P can be measured using a combination of challenging, low-throughput, and/or indirect techniques such as pressure chambers and pico-osmometers, cell pressure probes, picogauges or indenters (Beauzamy *et al.*, 2014; Knoblauch *et al.*, 2014; Boursiac *et al.*, 2022). Thus, there is a real need for improved tools and non-destructive techniques using, for example, chemical probes, protein reporters, or marker genes.

Here, we addressed the early stages of water deficit perception by considering that the drop in external Ψ would primarily provoke a change in either Π or P. Using hydroponically grown Arabidopsis plants that were osmotically challenged with permeating and non-permeating solutes, we first evaluated the impact of a drop in external Ψ on the P of root cortical cells. We then investigated root transcriptional regulations as a readout, to test whether Π or P can trigger specific and quantitative responses, a first step into the question whether Π or P can be genuinely perceived by plant cells.

Material and Methods

Plant material and culture conditions

All experiments were performed using *Arabidopsis thaliana* ecotype Col-0. Seeds were surface sterilized and kept at 4°C in dark until sowing on 1/2 Murashige and Skoog basal salt medium agar plates [2.2 $g.l^{-1}$ MS (Sigma), 1% sucrose (Euromedex), 0.05% MES (Euromedex), and 0.7% agar (Sigma), pH 5.7 adjusted using KOH]. For pre-germination, plates were incubated vertically in growth chamber under long-day conditions (16h/8h, 21°C, 60% humidity). After 10 days, seedlings were transferred to a hydroponic medium [1.25 mM KNO_3, 0.75 mM $MgSO_4$, 1.5 mM $Ca(NO_3)_2$, 0.5 mM KH_2PO_4, 50 µM Fe-EDTA, 50 µM H_3BO_3, 12 µM $MnSO_4$, 0.70 µM $CuSO_4$, 1 µM $ZnSO_4$, 0.24 µM MoO_4Na_2, 100 µM Na_2SiO_3] and further grown under the same culture conditions. Cell pressure probe measurements, transcriptomic analyses, and treatments for qPCR analysis were performed at 4- 8 days, 6 days, or 6-11 days after transfer, respectively.

Osmotic treatments

Osmotic stress treatments were performed using a hydroponic solution containing either 25mM-50mM-75mM-100mM NaCl (Sigma); 50mM-100mM-150mM sorbitol (Sigma); 75$g.l^{-1}$-100 $g.l^{-1}$-125 $g.l^{-1}$-150 $g.l^{-1}$ polyethylene glycol 8000 (Sigma); or 50mM-100mM-150mM-200mM ethylene glycol (Sigma). Table 1 recapitulates the solutions and their respective osmotic potential.

Cell Pressure Probe Measurements

Cell pressure probe measurements were performed as described previously (Javot *et al.*, 2003). Our device uses a pulled and beveled glass microcapillary (tip external diameter: 4 to 8µm), filled with mineral oil and mounted onto a pressure probe. Primary root tip segments of ~2-3cm were excised from Arabidopsis seedlings and laid on a filter paper perfused with hydroponic or treatment solution. Measurements were performed within a distance of 1cm from the elongation of the first root hairs. Data were recorded using an especially designed software (Pfloek; Department of Plant Ecology,

University of Bayreuth, Germany). Due to the dead volume of the system and the maximal speed of the peristaltic pump, it took approximatively 2min to fully change the perfusion solution around the root.

Transcriptomic analyses

Osmotic treatments were performed by transferring plants for 15 min into a hydroponic or treatment solution. The whole roots were harvested after 15 min of treatment and immediately frozen in liquid nitrogen. Each sample was a pool of three plants and two sets of plants were treated independently. Frozen samples were ground using a MM 400 mixer mill (Retsch). Total RNA was extracted using TRI Reagent (Molecular Research Center, Inc), DNA contamination was removed by digestion with DNase I (Promega), and further purification of the RNAs was performed using the MinElute Cleanup Kit (Qiagen), all according to the manufacturer's instructions. Concentration and purity of the RNAs was assessed by spectrophotometry and integrity was confirmed using RNA 6000 Nanochips with a 2100 Bioanalyzer (Agilent). Gene expression measurements were performed using Arabidopsis Affymetrix Gene1.1 ST array strips (Affymetrix). For each sample, 100 ng of total RNA was processed using the GeneChip WT PLUS Reagent Kit (Affymetrix) following the manufacturer's instructions. Hybridization on array strips was performed for 16h at 48°C. The arrays were washed, and stained, using GeneAtlas Hybridization, Wash and Stain Kit for WT Array Strips following the manufacturer's instructions. Array strips were scanned on the GeneAtlas system.

Microarrays raw data were processed with GCRMA available in the Expression Console Software package developed by Affymetrix. The Affymetrix Microarrays data have been deposited in the National Center for Biotechnology Information's Gene Expression Omnibus in compliance with Minimum Information About a Microarray Experiment standards (http://www.ncbi.nlm.nih.gov/geo/) and are accessible through Gene Expression Omnibus Series accession no. GSE223207.

Transcriptomic data analyses

The multi-way type II ANOVA model and one-way ANOVA analyses for genes expression correlation to Π and P were run in R (v.4.2.0). Thresholds for the selection of differentially expressed probes (DEPs) were adjusted by comparison of the p-values versus FDR corrected p-values and their frequency. A general cut-off of FDR < 0.2 was ruled out, which yielded non-adjusted p-values thresholds of 0.001 for the solutes (NaCl, Sorbitol, PEG and EG), and 0.0004 and 0.0012 for Π and P, respectively. A few genes were removed from the Π- and P-specific lists since they were associated to at least 2 probes and gave inconsistent ANOVA test results:

- Removed from "Π-specific genes": At1g72850, At1g78270, At2g24540, At2g33810, At4g13920, At4g24410, At4g25880, At4g26490,
- Removed from "P-specific genes": At1g07130, At1g07725, At1g08590, At1g51640, At1g56240, At1g72850, At2g11851, At2g22960, At3g22070, At3g54630, At3g56770, At4g24410, At4g28650, At4g36030, At4g38210, At4g38550, At5g59730.

Treatments clustering was obtained in RStudio (RStudio 2022.07.1+554) by calculating the Euclidean distance between treatments using the function *dist()*, then the clusters obtained by *hclust()* were plotted using *plot()*, with default values. Venn diagrams were elaborated with the nVennR package (Pérez-Silva *et al.*, 2018).

Semantic analysis of the clusters was performed using Genecloud (Krouk *et al.*, 2015) from m2sb.org webpage with an FDR threshold set to 1%. Gene ontology enrichment was performed in R using ClusterProfiler v.4.4.2 (Wu *et al.*, 2021) and org.At.tair.db (v3.15.1) for the Arabidopsis genome wide annotation database (Carlson, 2017). Lists overlaps scores were obtained using the Genesect algorithm from the Virtual Plant platform (Katari *et al.*, 2010).

RT-qPCR

RNA extraction was performed by using the Direct-zol RNA Miniprep Plus Kits from Zymo Research (NO.2072). cDNA solution was synthesized from 1 µg RNA and oligo-DT_{15}, dNTPs and M-MLV (Promega) according the manufacturer protocol. At1g13320 (PDF2) and At4g34270 (TIP41-like) were selected as internal normalizing genes, because of their stability in roots under abiotic stresses (Czechowski *et al.*, 2005). RT-qPCR primers were designed by using the primer3 online website (version 4.1.0, Table S1). RT-qPCR reactions were performed according to the procedure recommended by the manufacturer (Takara)(0.5 µL H2O, 0.25 µL F/R, 4 µL cDNA and 5 µL TAKARA SYBR premix Ex Taq. 95℃ for 30 s; 95℃ for 5 s, 60℃ for 30 s (40 cycles)). RStudio software was used to calculate gene expression according to Vandesompele's method (Vandesompele *et al.*, 2002).

mRNA decay analysis

The half-life time of mRNAs ($T_{1/2}$) was calculated from data available in Sorenson et al. 2018. It is based on the decay rate (α) modeled from RNAseq data upon cordycepin treatment on *sov* mutant seedlings (i.e. Col 0), and is calculated as $T_{1/2}= \ln(2)/\alpha$ (Sorenson *et al.*, 2018). $T_{1/2}$ of each mRNA from genes in the clusters are presented individually and as boxplots. The values above the boxplots correspond to a non-parametric estimation of the p-value of the $T_{1/2}$ of a given cluster being smaller than that of the whole genome. In this boostrap-based approach, the median $T_{1/2}$ of the cluster is compared to the median $T_{1/2}$ of a sample (of the same size) from the whole genome data. The number of occurrences

where the genome sample median $T_{1/2}$ is smaller than the cluster median $T_{1/2}$ divided by the number of tests realized (10^4 tests), aka the frequency, is reported.

Results

Turgor response of root cortical cells to osmotic challenges

We determined the P of root cortical cells with a cell pressure probe (Boursiac *et al.*, 2022) upon root perfusion with a standard hydroponic solution, or the same solution supplemented with various concentrations of distinct solutes: sodium chloride (NaCl), sorbitol, poly ethylene glycol 8000 (PEG), or ethylene glycol (EG) (Table 1). In contrast to others, the latter solute can significantly diffuse through cell membranes. Thus, EG is expected to concomitantly reduce the Ψ of the solution and cells, without significantly changing the Ψ gradients between compartments (Creelman and Zeevaart, 1985). Figures 1A-D show cortical cell pressure measurements over the course of approximately 30 min of a perfusion with various concentrations of NaCl, sorbitol, PEG and EG. For all treatments, we observed a progressive reduction in P, which reached a minimal value within 10 min. P remained stable for at least 10 additional minutes for most conditions except EG treatments, where a partial restoration of P was eventually observed. We averaged P within 10-20 min of treatment and represented it as a function of Π of the bathing solution (Figure 1E). For all solutes except EG, we observed a linear and relatively similar relationship between Π of the solution and cortical cell P. In the 10-20 min time range, EG provoked a reduction in P of ~0.1 MPa, independently of its concentration, and thereby of Π. Note that treatments were designed so that P remained positive in cortical cells, and hence cortical cells were not plasmolysed. These results suggest that root cortical cells behave as osmometers with the solutes except EG, and show no major osmotic regulation within the time frame of the experiment. The 15 min time-point, which corresponds to a mostly stable P, seems to be well-adapted to studying the early molecular events triggered by osmotic challenges.

Transcriptional response of roots osmotically challenged for 15min.

We treated Arabidopsis plants for 15 min using the various conditions tested above, and performed transcriptomic analyses on RNA extracted from their roots. This genome-wide investigation of gene expression in response to 15 distinct osmotic challenges (plus a control condition in which plants were transferred into an identical hydroponic solution, table 1) was recorded using Affymetrix A. thaliana genome arrays (Gene1.1 ST array strip, 2 independent biological experiments). We used the probes data from the genome array to perform a hierarchical classification of the osmotic challenges, and explore their convergence in transcriptional control (Figure 2A). A general feature is that most of the challenges were grouped by the nature of the solute (NaCl, Sorbitol, PEG or EG), suggesting that it

represents a main determinant of whole genome transcriptional status. EG treatments were clustered next to the hydroponic condition, which echoes to the limited effect of this solute on P. Treatments with the two highest PEG concentrations were also apart from the other challenges, which suggests that these conditions trigger responses of yet another type.

The data sets were then modeled through ANOVA with the following linear model:

$$Y_i = \alpha.NaCl_{factor} + \beta.\ Sorbitol_{factor} + \gamma.\ PEG_{factor} + \delta.EG_{factor}$$

where Y_i is the signal intensity of an ATH1 probe, α, β, γ, δ are coefficients representing the effect of each of the factors, respectively, and $NaCl_{factor}$, $Sorbitol_{factor}$, PEG_{factor} and EG_{factor} are factors indicating the concentration of each treatment (table 1, full results provided in supplemental data S1) (Ristova *et al.*, 2016). Note that this model uses partial regressions against factor that are derived from the concentration of the solutes. Importantly, the factors are set to 0 when another solute is used as a treatment and, as a consequence, are negatively impacting the score of genes which could be regulated by common underlying processes (such regulations are addressed in the next section). Note also that all solutes are included in the model, despite no co-treatment was performed and thus no interaction is investigated, in a bid to increase the statistical power. We then considered a probe as differentially expressed if its ANOVA p-value was significantly different at $p<0.001$ (FDR<0.2) for any of the 4 factors. 526 differentially expressed probes (DEPs), corresponding to 436 differentially expressed genes (DEGs) were retrieved with this analysis. In order to estimate the amplitude of the transcriptomic regulation, we first separated and sorted the DEPs according to the conditions in which they were regulated (Figure 2B). Probes regulated specifically by one solute only were the most represented. PEG was the solute with most specific impact, with 182 DEPs (159 DEGs). NaCl, sorbitol and EG treatments resulted in 127 (92), 68 (60) and 14 (12) specific DEPs (DEGs), respectively. The remaining 135 DEPs were regulated significantly in 2 or more solutes treatments (Figure 2B). Because DEGs could be either up or downregulated by the treatments, we separated the genes regulated by each specific solute in two clusters based on their averaged, centered, expression signal. Figure 2C visually confirms that the DEGs identified by this approach indeed exhibit a quantitative transcriptional regulation for a particular solute mostly.

Do Π or P trigger specific gene regulations?

Because all treatments share a common osmotic component (table 1), the transcriptional response can also be observed with the prism of a dose-dependent response to osmotic pressure. We therefore performed a one-way ANOVA on our transcriptomic data, using Π as the explanatory, continuous, variable (supplemental data S1). This analysis retrieved 72 DEGs. EG was also used forits capacity to

reduce the Ψ of the solution but, at variance of the other treatments, provoking only a limited reduction in P (Figure 1 D, E). With the aim of differentiating the effect of an osmotic treatment on the transcriptome through either the osmotic potential or its impact on P, we performed a similar one-way ANOVA analysis of the 15 min transcriptomic response to the treatments, but with P as the explanatory variable (supplemental data S1). This analysis resulted in 179 DEGs. While 53 DEGs were identified in both Π and P response (see discussion), 19 and 126 DEGs were specific of Π and P, respectively (Figure 3A). Each group of Π or P DEGs was split in 2 clusters, in order to account for potential up- and down-regulations. For the Π-specific genes, the mRNA abundance of the DEGs appeared to be regulated quantitatively for all solutes employed (Figure 3B, upper panels), while a similar regulation for NaCl, sorbitol and PEG, but not EG, was observed for the P-specific genes (Figure 3B, lower panels). Most importantly, a clear quantitative correlation to Π or P was confirmed for the Π-specific (Figure 3C) and P-specific (Figure 3D) DEGs, respectively. Altogether, our transcriptomic approach suggests that while cells remain turgid, at least two components of the osmotic treatment, P and the Π of the bathing solution, are able to provoke specific quantitative responses of the transcriptome, resulting in both up- and down-regulations.

Are promoter activity and mRNA decay pathways involved in the Π or P transcriptional regulation?

The 1Kb promoter regions of the DEGs were analyzed using the MEME suite (Bailey *et al.*, 2015; Grant and Bailey, 2021, Preprint). Both new and already known (O'Malley *et al.*, 2016) enriched motives were considered for Π–cluster 1 or the P-specific clusters (with only 4 genes, the Π-cluster 2 was not analyzed, supplemental data S2, S3A-C). All clusters showed an enrichment in motives (or similar motives) known to bind ABI3VP1 transcription factors (TFs). All other motives were found enriched in 1 cluster only: REM, C2C2dof and BBRBPC binding elements for P-cluster 2, C2H2 and ZFHD binding motives for P-cluster 1, and an ARID binding motif for Π–cluster 1.

We also considered whether the regulation of the mRNA abundance of the DEGs could be post-transcriptional, and in particular due to their degradation. Using the transcription inhibitor cordycepin and a model-assisted RNAseq approach, Sorenson et al. (2018) performed a global evaluation of mRNA decay rates in Arabidopsis and evaluated the implication of the three main decay pathways (Sorenson *et al.*, 2018). As a first hint into this type of regulation for the DEGs identified herein, we used the mRNA decay rates obtained in the above-mentioned study, for the *sov* Col genotype, to calculate the mRNA half-life of our genes of interest in their growth conditions ($T_{1/2}$). The median $T_{1/2}$ of all mRNAs detected in this study was around 101 min. The median $T_{1/2}$ calculated for genes of the Π-specific clusters and P-specific cluster 2 were significantly lower, with mean values of 56 min, 23 min and 69 min, respectively (Figure 4), and was not different for genes of P-specific cluster 1.

A short list of Π or P correlated genes

In a bid to confirm the robustness of the microarray approach, and select potentially good candidates that could serve as markers of P or Π, we ranked genes of the 4 categories (Π– or P-specific, up or downregulated) according to 3 parameters: the adjusted R square of a linear fit of their averaged centered expression as a function of Π or P, the slope of the linear fit, and the average expression level in control conditions (Supplemental data S4). We randomly selected a few genes, among the best ranked of each list, to confirm their regulation by RT-qPCR, upon 15min NaCl, sorbitol and EG treatments, and in three new, independent, biological replicates. Figure 5 shows plots of the comparison between the means of the microarray signals and of the signals obtained by RT-qPCR. 10 genes out of 12 displayed a significant correlation between both signals, thus globally confirming the results obtained by the microarray approach. The Π-specific cluster 2 showed poor reliability, with only 1 gene out of 3 having a similar behavior upon confirmation by RT-qPCR and in new biological replicates. The P-specific cluster 1 exhibited the highest rate of confirmation, in both the p-value of the correlation and the R^2 of the relationship. Among them, At1g64640 stood out with a correlation p-value below 1e-3 and a R^2 >0.9. The expression of this gene is therefore robustly and quantitatively correlated to P, at 15 min after an osmotic challenge.

What are the gene functions altered by Π or P?

A semantic analysis of the gene annotation present in the 4 clusters (Π– or P-specific, up or down-regulated) using Genecloud (Krouk *et al.*, 2015) revealed that the Π-specific clusters do not show any particular semantic enrichment. Arabinogalactan, Cys/His rich proteins, “protein kinase C” and TFs related terms were detected in the cluster 1 of P-specific genes (Figure 6A, left). Cluster 2 of P-specific genes showed enrichments in terms related to ethylene-dependent and other transcriptional regulations as well as defense responses (Figure 6A, right).

A Gene Ontology (GO) enrichment analysis was also performed. Π-specific cluster 1 was found specifically enriched in genes associated with defense responses and the cell wall (Figure 6B, left). Results for P-specific clusters were quite consistent with the semantic analysis. P-specific cluster 1 was enriched in “anchored components” which echoes to the arabinogalactan term above (not shown). P-specific cluster 2 was enriched in terms associated to ethylene and defense responses. In a bid to sharpen the above mentioned GO analysis, we also evaluated the overlap between our gene lists and the Gene Ontology list “response to NaCl” (GO:0009651) as well as two of the upstream terms: “response to abiotic stress” (GO:0009628) and “response to stimulus” (GO:0050896) (Figure 6C). The two upregulated clusters, Π-specific cluster 1 and P-specific cluster 2, showed a significant overlap with the genes in the categories “response to stimulus” and “response to abiotic stress”, but not with

"response to salt stress", indicating the convergence of our approach to the existing knowledge. Because the specificity of the response might not prevail under short term treatment, and a general stress response (GSR) may rather be activated (Bjornson *et al.*, 2021), we also compared our lists to the genes identified as GSR from the work of Ma and Bohnert (2007). In this study, the authors analyzed a collection of transcriptome profiles of plants under various treatments, and highlighted a stress-dependent cluster that could represent cell-level stress responses (Ma and Bohnert, 2007). Π-specific cluster 1 and P-specific cluster 2 showed a significant overlap with the GSR genes, with a greater Z-score than for the previous comparisons (Figure 6C). This analysis suggests that some of the upregulated genes that are quantitatively (and inversely) correlated to Π or P belong to a common and early response to stresses.

Finally, our candidates were also compared to a list of genes encoding transcription factors (Pruneda-Paz *et al.*, 2014), and showed no significant enrichment in this category of genes (Figure 6C).

Discussion

This study was designed to improve our comprehension of which component of a water deficit can be perceived by plant roots. For this, we considered both the Π of the bathing solution or the P of root cells as possible input signals (Figure 1) and used whole genome transcriptional responses as a readout. The approach was meant to unravel any quantitative relationship between the input signals and responses.

Parameters at the origin of the transcriptional responses

In addition to solute specific transcriptional responses (Figure 2D), our study unraveled 72 genes which expression correlated to Π, independently of the solute used (Π-specific clusters, Figure 3, A and C). These results suggest that plant cells have the capacity to sense and transduce the external osmotic potential. Measurement with a cell pressure probe allowed us to also look for correlations between gene expression and the P of root cortical cells. In this approach, the use of EG as a permeating osmoticum was critical to make a distinction between the effects of the solutes on P and Π (Figure 1E). 241 genes were found to be truly correlated to P (P cluster 1 and 2, Figure 3, A and D) and suggest that plant cells also have the capacity to specifically sense and respond to the internal pressure. Due to the experimental design and variability, 53 genes could not be assigned to a Π– or P-specific response (Figure 3A) and would deserve more investigation, in particular with the use of other permeating solutes. Nevertheless, the identification of genes which expression is quantitatively correlated to all possible combinations (Π or P, up- or down-regulation) highlights the multiplicity of water deficit responses in plant cells. Since we uncovered potentially distinct regulatory mechanisms, our results

will help clarifying studies on mechano- and osmo-sensing as well as our understanding of plant response to water deficit. For example, turgor recovery upon plant adaptation to low external water potential by solutes synthesis/accumulation necessarily implies an uncoupling between P and Π.

Π or P may not be the exact physico-chemical parameters that are genuinely perceived by plants. It has been suggested that, in leaves, accumulation of ABA is triggered by a drop in relative water content (RWC) rather than variations in P or Π (Jia *et al.*, 2001; Sack *et al.*, 2018). This distinction was made possible by experiments of leaf dehydration beyond the turgor point loss. In our experiments, turgor was preserved because we anticipated that plasmolysis could trigger distinct responses and, on a crude assumption, the relative change in cell volume ($\Delta V/V$) is linearly correlated to the variation in P (ΔP) according to $\Delta P = \varepsilon . \Delta V/V$ where ε stands for the cell wall elastic modulus (Hüsken *et al.*, 1978). Thus, we cannot differentiate P or RWC and may use them interchangeably in our interpretations. It would also be interesting to establish whether the internal (intracellular) osmotic potential (Π_{int}) can be sensed and trigger specific transcriptional responses. Because cells behave as osmometers in the presence of NaCl, sorbitol and PEG, Π_{int} can be expressed, at equilibrium, as $\Pi_{int} = \Pi + P$. Since the effects on Π and P were close (Figure 1E), those solutes do not allow to distinguish Π_{int} from Π. EG flux was not completely equilibrated after a 15min treatment (Figure 1D), and Π_{int} could be calculated based on equations that describe P variations in cells perfused with a permeating solute (Steudle, 1989). However, experimental variations did not allow us to reach a sufficient resolution of the hydraulic and solute relaxation phases in cells under EG treatment. Thus, our current study cannot conclude on the ability of root cells to respond to changes in Π_{int}.

Finally, we would like to point other kinds of avenues for interpreting our data. Firstly, Π changes are isotropic in the hydroponic solution, so that all root parts were somewhat homogeneously challenged. In contrast, P, which was only measured in resting cortical cells, close to root tip, may be different in other cell types. For example, epidermal cells of Arabidopsis roots usually show a P that is about 0.1MPa lower than that of cortical cells (Javot *et al.*, 2003). This difference translates into a shift in the response curve of P to Π and could eventually lead to plasmolysis, in a limited number of cell types, and under the most severe osmotic challenges. Secondly, gene expression data were obtained from a whole root mRNA extraction, and could mask cell-type specific regulations which are known to exist (Ma and Bohnert, 2007; Dinneny *et al.*, 2008). Finally, the transcriptome status at 15min is the consequence of regulatory mechanisms that were activated within the first 10 min, where turgor pressure was in a transient status. A more detailed kinetic of the early events would shed light on the gene regulatory networks (Krouk *et al.*, 2010) activated very early by Π or P variations. All these aspects

deserve more investigations at the cell, gene and genome levels, for which our current work provide a well-defined framework.

Mechanisms of mRNA abundance regulation by Π or P

In this study, mRNA abundance, as monitored by microarrays or RT-qPCR, was employed as a readout of water deficit signaling. We realize that changes in a mRNA abundance can be due to many molecular aspects acting on their synthesis or decay. We gathered informations for two of them: the corresponding promoter activity and its RNA degradation.

We first analyzed the promoters of genes in the Π– or P-specific clusters for the presence of binding sites for putative TFs that could regulate their expression at the transcriptional level (Sup data S3 and S4). We mostly identified binding sites for TFs belonging to the C2C2dof, ABI3VP1, BBR/BPC, C2H2, ZFHD, and REM families. Members of these families have been involved in a broad range of processes but are not specific of water deficit (Yamaguchi-Shinozaki and Shinozaki, 2006; Coutand *et al.*, 2009; Noguero *et al.*, 2013; Mantegazza *et al.*, 2014; Taylor-Teeples *et al.*, 2015; Perrella *et al.*, 2018; Lai *et al.*, 2021; Yan *et al.*, 2021; Wang *et al.*, 2022). This result corroborates the idea that a multiplicity of TFs can regulate each gene. It also indicates that the short-term responses to both Π and P likely occur through transcriptional regulation, for which we could not identify representative motives nor the critical role of specific TFs.

To address a possible role of mRNA degradation, we referred to a previous work that studied mRNA decay, but under control conditions (Sorenson *et al.*, 2018). With a median $T_{1/2}$ of >100 min at the whole genome level, we hypothesized that a short $T_{1/2}$ in resting conditions might be a prerequisite for genes we identified as down-regulated within 15 min by the osmotic treatments (Π cluster 2 and P cluster 1, Figures 3 and 4). Indeed, the relatively short $T_{1/2}$ calculated for genes of Π-specific cluster 2, together with a promoter activity arrest, is compatible with the regulation we observed. Conversely, this may not be the case for genes of P cluster 1 which showed a median $T_{1/2}$ similar to that of the whole genome. Here, we speculate that on top of a down-regulation of their promoter activity, a reduction in their $T_{1/2}$ should be induced by the osmotic challenges, thereby leading to their rapid downregulation. Indeed, phosphorylation of proteins of the mRNA decapping complex is regulated by osmotic stresses (Sieburth and Vincent, 2018). The multiplicity of Π or P responses that we identified therefore seems to translate into a similar complexity of mRNA regulation mechanisms, and provides an interesting avenue for further investigation.

Functions regulated by Π or P

Our approach could possibly identify genes which function in Π or P signaling. Semantic and gene ontology enrichments were performed on the gene lists and identified complementary terms. Generic terms retrieved by this approach were mainly associated to transcriptional regulation, responses to abiotic or biotic stimuli, and the cell wall (Figure 6A and B). It is difficult to extract any precise signaling pathway here since many annotations of these genes are inferred, and some of the terms define diverse functions. For example, arabinogalactan proteins are involved in many processes in roots including biotic and abiotic responses (Hromadová *et al.*, 2021), and genes of the C1-like domain superfamily have been associated to various biological/developmental processes, including root epidermal cell differentiation (Bruex *et al.*, 2012). It is also somehow surprising to extract terms related to biotic stresses and defense responses. However, this may result from genes whose annotation originates from, but not necessarily restricts to, "biotic" conditions, or whose function was only indirectly inferred. Indeed, our approach uncovers genes associated to the "short-term", less specific, general stress response (Figure 6C)(Bjornson *et al.*, 2021). Importantly, we introduce here the notion that there is a quantitative relationship between the mRNA abundance of these genes and physico-chemical parameters (Figure 3C).

Quantitative responses to physico-chemical parameters

Our study integrates into earlier works focused on the perception of the physico-chemical conditions of cells. We investigated here the dose dependent effects of physico-chemical parameters on the root transcriptome. Such an approach has been successfully applied in poplar, where it was shown that the abundance of ZFP2 mRNA is correlated to the sum of strains upon stem bending (Coutand *et al.*, 2009), and which initiated great advances on the understanding of thigmomorphogenesis. With respect to water, a study was performed in sunflower where a generalized linear model fed by the expression level of 3 genes was developed in order to compute integrated parameters such as the pre-dawn water potential or the soil water content (Marchand *et al.*, 2013). There is a gap between obtaining correlations between physico-chemical parameters and gene expression –such as what we present here, and creating biomarkers or biosensors (Jones, 2014). Nevertheless, the genes identified in the 4 clusters could serve as molecular reporters to investigate the perception and signaling of Π or P. Indeed, this has been successfully achieved for temperature sensing, where the promoter of HSP70 was used as a quantitative reporter of ambient temperature, and allowed to discover the role of H2A.Z proteins in the temperature-dependent modulation of transcription (Kumar and Wigge, 2010).

Conclusion

Thanks to a combination of physiological techniques and a transcriptome approach, we showed the existence of rapid, specific transcriptional responses to water-related physico-chemical parameters.

We propose herein a list of early responsive genes whose mRNA abundance in quantitatively correlated to external Π or to cell P. This list provides potential reporter genes that could serve to elaborate biomarkers of the plant cells water status. This study also paves the way for future dissection of the molecular perception of water deficit in plants, through the identification of how their mRNA abundance is regulated.

Supplementary data

Table S1: primers sequences for the RT-qPCR analysis

Supplemental data S1: p-values of the ANOVA analyses and probe/AGI correspondence for the Gene1.1 ST array

Supplemental data S2: summary of TFs binding sites enrichment in the Π and P clusters

Supplemental data S3 A, B, C: output of the promoter analysis for each cluster

Supplemental data S4: gene list of each cluster, highlighting the genes that were tested further by RT-qPCR

Acknowledgements

We thank Alexandre Martinière, François Parcy and François Tardieu for helpful discussions, and Cécile Fizames for help in the promoter analysis. We thank 2 anonymous reviewers for helping us improve this manuscript.

Authors contributions

YB and GK conceptualized the research. AC and YH performed the research with contributions from TB for physiological measurements. YH, GK and YB analyzed the data with contributions from SR and CM. YB wrote the article with insights from CM. All authors contributed to reviewing the manuscript and agreed to its content.

Funding

This project was funded through Labex AGRO 2011-LABX-002, project number 1403-012 to YB, in the I-Site Muse framework, coordinated by Agropolis Fondation, and by the CNRS through the MITI interdisciplinary programs (“Turgomap” to YB). YH is supported by the China Scholarship Council. TB is supported by the LabEx NUMEV (ANR-10-LABX-0020) within the I-Site MUSE (ANR-16-IDEX-0006) and by Region Occitanie.

Conflict of interest

None declared

Data availability

The transcriptomic data that support the findings of this study are openly available in Gene Expression Omnibus Series (http://www.ncbi.nlm.nih.gov/geo/) GSE223207.

The code and source files (besides transcriptomic data) used to analyze the data and/or to generate the figures 1 to 5 of this study can be downloaded from https://github.com/ybinrae/Watermarker_paper1.git .

References

Bailey TL, Johnson J, Grant CE, Noble WS. 2015. The MEME Suite. Nucleic Acids Research **43**, W39-49.

Beauzamy L, Nakayama N, Boudaoud A. 2014. Flowers under pressure: ins and outs of turgor regulation in development. Annals of Botany **114**, 1517–1533.

Bjornson M, Pimprikar P, Nürnberger T, Zipfel C. 2021. The transcriptional landscape of Arabidopsis thaliana pattern-triggered immunity. Nature Plants **7**, 579–586.

Boursiac Y, Protto V, Rishmawi L, Maurel C. 2022. Experimental and conceptual approaches to root water transport. Plant and Soil **478**, 349–370.

Bowler MG. 2017. The physics of osmotic pressure. European Journal of Physics **38**, 055102.

Bruex A, Kainkaryam RM, Wieckowski Y, *et al.* 2012. A Gene Regulatory Network for Root Epidermis Cell Differentiation in Arabidopsis. PLOS Genetics **8**, e1002446.

Carlson M. 2017. org.At.tair.db.

Coutand C, Martin L, Leblanc-Fournier N, Decourteix M, Julien J-L, Moulia B. 2009. Strain Mechanosensing Quantitatively Controls Diameter Growth and PtaZFP2 Gene Expression in Poplar. Plant Physiology **151**, 223–232.

Creelman RA, Zeevaart JAD. 1985. Abscisic Acid Accumulation in Spinach Leaf Slices in the Presence of Penetrating and Nonpenetrating Solutes. Plant Physiology **77**, 25–28.

Czechowski T, Stitt M, Altmann T, Udvardi MK, Scheible W-R. 2005. Genome-Wide Identification and Testing of Superior Reference Genes for Transcript Normalization in Arabidopsis. Plant Physiology **139**, 5–17.

Dinneny JR, Long TA, Wang JY, Jung JW, Mace D, Pointer S, Barron C, Brady SM, Schiefelbein J, Benfey PN. 2008. Cell Identity Mediates the Response of Arabidopsis Roots to Abiotic Stress. Science **320**, 942–945.

Grant CE, Bailey TL. 2021. XSTREME: Comprehensive motif analysis of biological sequence datasets. bioRxiv.

Hamant O, Haswell ES. 2017. Life behind the wall: sensing mechanical cues in plants. BMC Biology **15**, 59.

Haswell ES, Verslues PE. 2015. The ongoing search for the molecular basis of plant osmosensing. Journal of General Physiology **145**, 389–394.

Hromadová D, Soukup A, Tylová E. 2021. Arabinogalactan Proteins in Plant Roots – An Update on Possible Functions. Frontiers in Plant Science **12**.

Hüsken D, Steudle E, Zimmermann U. 1978. Pressure Probe Technique for Measuring Water Relations of Cells in Higher Plants. Plant Physiology **61**, 158–163.

Javot H, Lauvergeat V, Santoni V, *et al.* 2003. Role of a Single Aquaporin Isoform in Root Water Uptake. Plant Cell **15**, 509–522.

Jia W, Zhang J, Liang J. 2001. Initiation and regulation of water deficit-induced abscisic acid accumulation in maize leaves and roots: cellular volume and water relations. Journal of Experimental Botany **52**, 295–300.

Jones HG. 2014. The use of indirect or proxy markers in plant physiology. Plant, Cell & Environment **37**, 1270–1272.

Katari MS, Nowicki SD, Aceituno FF, *et al.* 2010. VirtualPlant: A Software Platform to Support Systems Biology Research. Plant Physiology **152**, 500–515.

Knoblauch J, Mullendore DL, Jensen KH, Knoblauch M. 2014. Pico Gauges for Minimally Invasive Intracellular Hydrostatic Pressure Measurements. Plant Physiology **166**, 1271–1279.

Krouk G, Carré C, Fizames C, Gojon A, Ruffel S, Lacombe B. 2015. GeneCloud Reveals Semantic Enrichment in Lists of Gene Descriptions. Molecular Plant **8**, 971–973.

Krouk G, Mirowski P, LeCun Y, Shasha DE, Coruzzi GM. 2010. Predictive network modeling of the high-resolution dynamic plant transcriptome in response to nitrate. Genome Biology **11**, R123.

Kumar SV, Wigge PA. 2010. H2A.Z-Containing Nucleosomes Mediate the Thermosensory Response in Arabidopsis. Cell **140**, 136–147.

Lai W, Zhu C, Hu Z, Liu S, Wu H, Zhou Y. 2021. Identification and Transcriptional Analysis of Zinc Finger-Homeodomain (ZF-HD) Family Genes in Cucumber. Biochemical Genetics **59**, 884–901.

Ma S, Bohnert HJ. 2007. Integration of Arabidopsis thaliana stress-related transcript profiles, promoter structures, and cell-specific expression. Genome Biology **8**, R49.

Mantegazza O, Gregis V, Mendes MA, Morandini P, Alves-Ferreira M, Patreze CM, Nardeli SM, Kater MM, Colombo L. 2014. Analysis of the arabidopsis REM gene family predicts functions during flower development. Annals of Botany **114**, 1507–1515.

Marchand G, Mayjonade B, Varès D, *et al.* 2013. A biomarker based on gene expression indicates plant water status in controlled and natural environments. Plant, Cell & Environment **36**, 2175–2189.

Maurel C, Nacry P. 2020. Root architecture and hydraulics converge for acclimation to changing water availability. Nature Plants **6**, 744–749.

Noguero M, Atif RM, Ochatt S, Thompson RD. 2013. The role of the DNA-binding One Zinc Finger (DOF) transcription factor family in plants. Plant Science **209**, 32–45.

O'Malley RC, Huang SC, Song L, Lewsey MG, Bartlett A, Nery JR, Galli M, Gallavotti A, Ecker JR. 2016. Cistrome and Epicistrome Features Shape the Regulatory DNA Landscape. Cell **165**, 1280–1292.

Pérez-Silva JG, Araujo-Voces M, Quesada V. 2018. nVenn: generalized, quasi-proportional Venn and Euler diagrams. (J Wren, Ed.). Bioinformatics **34**, 2322–2324.

Perrella G, Davidson MLH, O'Donnell L, Nastase A-M, Herzyk P, Breton G, Pruneda-Paz JL, Kay SA, Chory J, Kaiserli E. 2018. ZINC-FINGER interactions mediate transcriptional regulation of hypocotyl growth in Arabidopsis. Proceedings of the National Academy of Sciences **115**, E4503–E4511.

Pruneda-Paz JL, Breton G, Nagel DH, Kang SE, Bonaldi K, Doherty CJ, Ravelo S, Galli M, Ecker JR, Kay SA. 2014. A Genome-Scale Resource for the Functional Characterization of Arabidopsis Transcription Factors. Cell Reports **8**, 622–632.

Ristova D, Carré C, Pervent M, *et al.* 2016. Combinatorial interaction network of transcriptomic and phenotypic responses to nitrogen and hormones in the Arabidopsis thaliana root. Science Signaling **9**, rs13–rs13.

Sack L, John GP, Buckley TN. 2018. ABA Accumulation in Dehydrating Leaves Is Associated with Decline in Cell Volume, Not Turgor Pressure. Plant Physiology **176**, 489–495.

Scharwies JD, Dinneny JR. 2019. Water transport, perception, and response in plants. Journal of Plant Research **132**, 311–324.

Sieburth LE, Vincent JN. 2018. Beyond transcription factors: roles of mRNA decay in regulating gene expression in plants. F1000Research **7**, F1000 Faculty Rev-1940.

Sorenson RS, Deshotel MJ, Johnson K, Adler FR, Sieburth LE. 2018. *Arabidopsis* mRNA decay landscape arises from specialized RNA decay substrates, decapping-mediated feedback, and redundancy. Proceedings of the National Academy of Sciences **115**, E1485–E1494.

Steudle E. 1989. Water flow in plants and its coupling to other processes: An overview. Biomembranes Part U: Cellular and Subcellular Transport: Eukaryotic (Nonepithelial) Cells. Methods in Enzymology. Academic Press, 183–225.

Taylor-Teeples M, Lin L, de Lucas M, *et al.* 2015. An Arabidopsis gene regulatory network for secondary cell wall synthesis. Nature **517**, 571–575.

Vandesompele J, De Preter K, Pattyn F, Poppe B, Van Roy N, De Paepe A, Speleman F. 2002. Accurate normalization of real-time quantitative RT-PCR data by geometric averaging of multiple internal control genes. Genome Biology **3**, research0034.1.

Verslues PE, Bailey-Serres J, Brodersen C, *et al.* 2023. Burning questions for a warming and changing world: 15 unknowns in plant abiotic stress. The Plant Cell **35**, 67–108.

Wang Z, Wong DCJ, Chen Z, Bai W, Si H, Jin X. 2022. Emerging Roles of Plant DNA-Binding With One Finger Transcription Factors in Various Hormone and Stress Signaling Pathways. Frontiers in Plant Science **13**.

Wu T, Hu E, Xu S, *et al.* 2021. clusterProfiler 4.0: A universal enrichment tool for interpreting omics data. The Innovation **2**, 100141.

Yamaguchi-Shinozaki K, Shinozaki K. 2006. Transcriptional regulatory networks in cellular responses and tolerance to dehydration and cold stresses. Annual Review of Plant Biology **57**, 781–803.

Yan J, Liu Y, Yang L, He H, Huang Y, Fang L, Scheller HV, Jiang M, Zhang A. 2021. Cell wall β-1,4-galactan regulated by the BPC1/BPC2-GALS1 module aggravates salt sensitivity in Arabidopsis thaliana. Molecular Plant **14**, 411–425.

569 # Tables

570 **Table 1: Summary of the osmotic treatments applied to the roots, and the factors of the ANOVA**
571 **model.**

572 Solutes were dissolved in the hydroponic solution. The osmotic potential of the solution was measured
573 at 20°C with an osmometer (Wescor), 3 digits after the decimal point are shown. The osmotic potential
574 is the opposite of the osmotic pressure.

Solute	Concentration (mM, g/l for PEG)	Π	P_{cort}	$NaCl_{factor}$	$Sorbitol_{factor}$	PEG_{factor}	EG_{factor}
None	0	0.021	0.41	0	0	0	0
NaCl	25	0.117	0.32	25	0	0	0
	50	0.238	0.25	50	0	0	0
	75	0.355	0.14	75	0	0	0
	100	0.425	0.05	100	0	0	0
Sorbitol	50	0.134	0.32	0	50	0	0
	100	0.255	0.18	0	100	0	0
	150	0.370	0.1	0	150	0	0
Polyethylene	75	0.073	0.31	0	0	75	0
glycol 8000	100	0.131	0.26	0	0	100	0
	125	0.209	0.2	0	0	125	0
	150	0.280	0.14	0	0	150	0
Ethylene Glycol	50	0.151	0.3	0	0	0	50
	100	0.268	0.29	0	0	0	100
	150	0.394	0.29	0	0	0	150
	200	0.516	0.26	0	0	0	200

575
576

Figure legends

Figure 1: Osmotic treatments reduce the P of root cortical cells in Arabidopsis.

A portion of ~3cm of root of 21 day-old plants, laid on a perfused Whatman paper, was treated with various solutes at different concentrations. Cortical cell P was measured with a cell pressure probe. **A to D**: measurement kinetics performed on plants treated with NaCl at concentrations of 0, 25, 50, 75, 100mM (the darker the color, the more concentrated, n>2 for each treatment), sorbitol at 50, 100 and 150mM, PEG8000 at 75, 100, 125 and 150 $g.l^{-1}$, and EG at 50, 100, 150 and 200mM, respectively. Zero in the time axis indicates the change in perfusion from hydroponic solution to the same solution complemented with treatments. A lowess smoothing was added in order to highlight the general behavior of P after each treatment **E**: plot recapitulating the measurements of P within the 10-20min time frame as a function of the osmotic pressure of the solution (average value ± SEM, n ≥ 2, blue: sorbitol, pink: NaCl, green: PEG, red: EG).

Figure 2: Features of the early transcriptomic response to osmotic treatments.

A: Dendrogram illustrating the effects of the solute nature and concentration on the regulation of gene expression. **B:** number of DEPs classified according to the solute used for the treatment. The matrix below indicates if those DEPs were found for a single or for various solute(s). **C:** Gene expression signals in the different treatments. Genes regulated by one solute only were selected from B and split in 2 clusters. The average, centered, expression value for each gene is plotted against the combination of solutes and concentrations used in the transcriptomic approach.

Figure 3: Correlations between gene expression and osmotic or turgor pressure.

A: Venn diagram showing the number of genes, in the same transcriptomic approach as in figure 2, which expression is significantly correlated to Π, P, or both. **B:** The 137 "Π-specific" genes and 401 "P-specific" genes were split in 2 clusters each, and their average centered expression is expressed as a function of the solute/treatment combination corresponding to the biological assays of the transcriptome approach. **C:** The 137 "Π-specific" genes were separated into 2 clusters and their average centered expression is expressed as a function of the osmotic potential of the solution of treatment, or the cortical cell turgor pressure. **D:** same representation as in C but for the 401 "P-specific" genes.

Figure 4: mRNA half-life time is reduced in 3 clusters in control conditions.

The half-life time of mRNAs ($T_{1/2}$) was calculated from Sorenson et al. 2018, based on the decay rate (α) modeled upon cordycepin treatment on *sov* mutant seedlings (i.e. Col 0, $T_{1/2}= \ln(2)/\alpha$) (Sorenson *et al.*, 2018). $T_{1/2}$ of each mRNA from genes in the clusters are presented individually and as boxplots. The numbers above the boxplots correspond the p-value of a bootstrap based test of $T_{1/2}$ of the cluster being smaller than the whole genome median $T_{1/2}$ (see M&M).

Figure 5: RT-qPCR validation of osmotic or turgor pressure clusters.

The expression of three candidates per list: Π or P, clusters 1 and 2 were investigated by RT-qPCR in 3 independent biological replicates. The plants were harvested 15min after transfer into a hydroponic solution, or the solution complemented with 25, 50,75, 100mM NaCl, or 50, 100, 150mM Sorbitol, or 50, 100, 150, 200g.l^{-1} EG. For each gene, normalized RT-qPCR signal (± SEM) is expressed as a function of the averaged signal (± SEM) obtained from the transcriptome analysis. The p-value of a correlation test (Pearson) as well as the linear fit (with its R^2 value) between the average values are indicated for each gene.

Figure 6: classification of the Π and P correlated genes.

A: output of the Genecloud semantic analysis for the 2 clusters showing a significant enrichment. **B:** Output of a gene ontology analysis for the 2 clusters showing significant enrichments in GO terms. The GO terms, gene counts for each GO term and adjusted p-value of the enrichment are presented. **C:** Degree of overlap (Z-score) between our genes lists and public genes lists related to osmotic stress, the general stress response, and a list of transcription factors, using the Genesect algorithm.

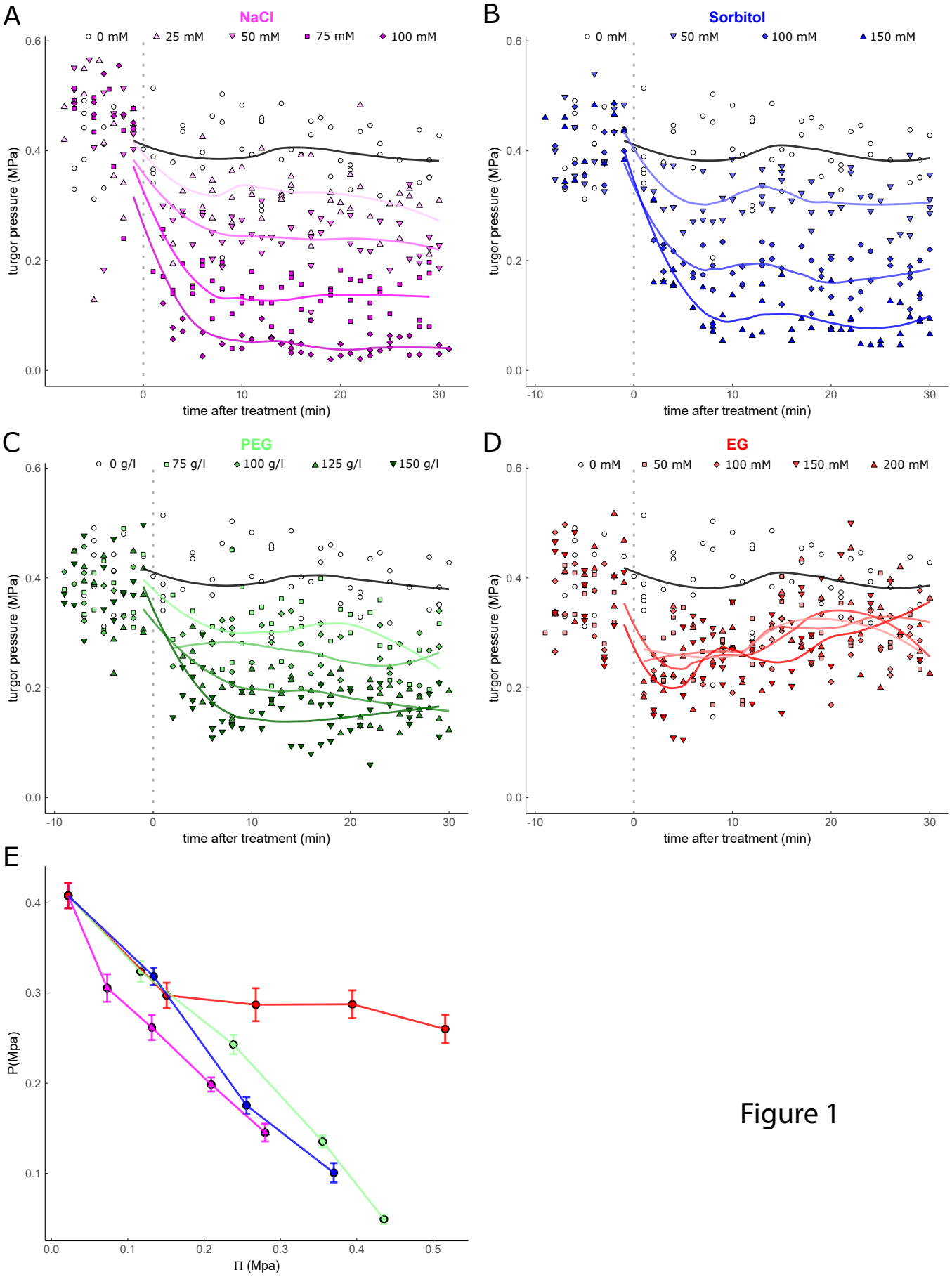

Figure 1

A portion of ~3cm of root of 21 day-old plants, laid on a perfused Whatman paper, was treated with various solutes at different concentrations. Cortical cell P was measured with a cell pressure probe. A to D: measurement kinetics performed on plants treated with NaCl at concentrations of 0, 25, 50, 75, 100mM (the darker the color, the more concentrated, n>2 for each treatment), sorbitol at 50, 100 and 150mM, PEG8000 at 75, 100, 125 and 150 g.l-1, and EG at 50, 100, 150 and 200mM, respectively. Zero in the time axis indicates the change in perfusion from hydroponic solution to the same solution complemented with treatments. A lowess smoothing was added in order to highlight the general behavior of P after each treatment E: plot recapitulating the measurements of P within the 10-20min time frame as a function of the osmotic pressure of the solution (average value ± SEM, n ≥ 2, blue: sorbitol, pink: NaCl, green: PEG, red: EG).

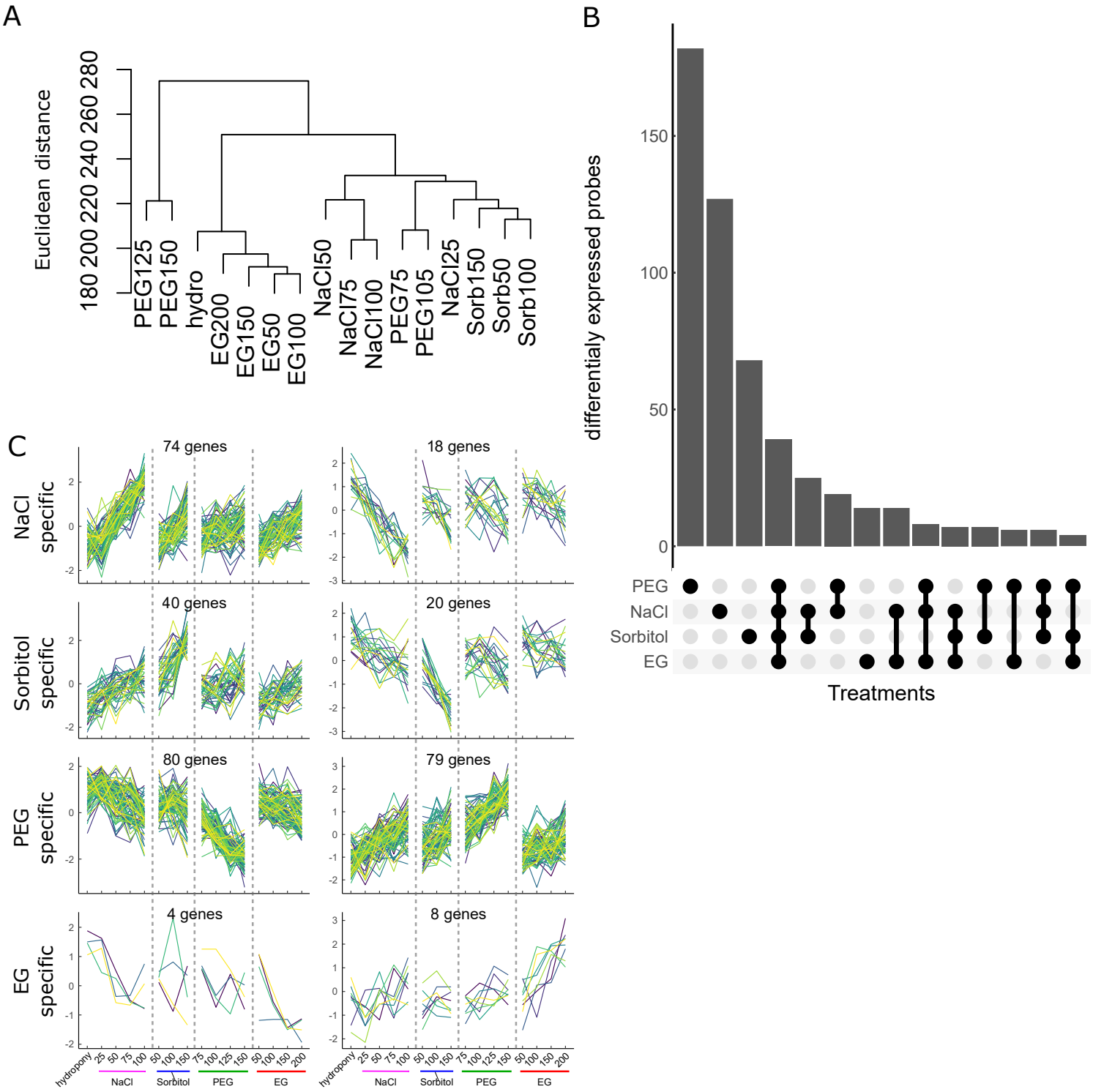

Figure 2

A: Dendrogram illustrating the effects of the solute nature and concentration on the regulation of gene expression. B: number of DEPs classified according to the solute used for the treatment. The matrix below indicates if those DEPs were found for a single or for various solute(s). C: Gene expression signals in the different treatments. Genes regulated by one solute only were selected from B and split in 2 clusters. The average, centered, expression value for each gene is plotted against the combination of solutes and concentrations used in the transcriptomic approach.

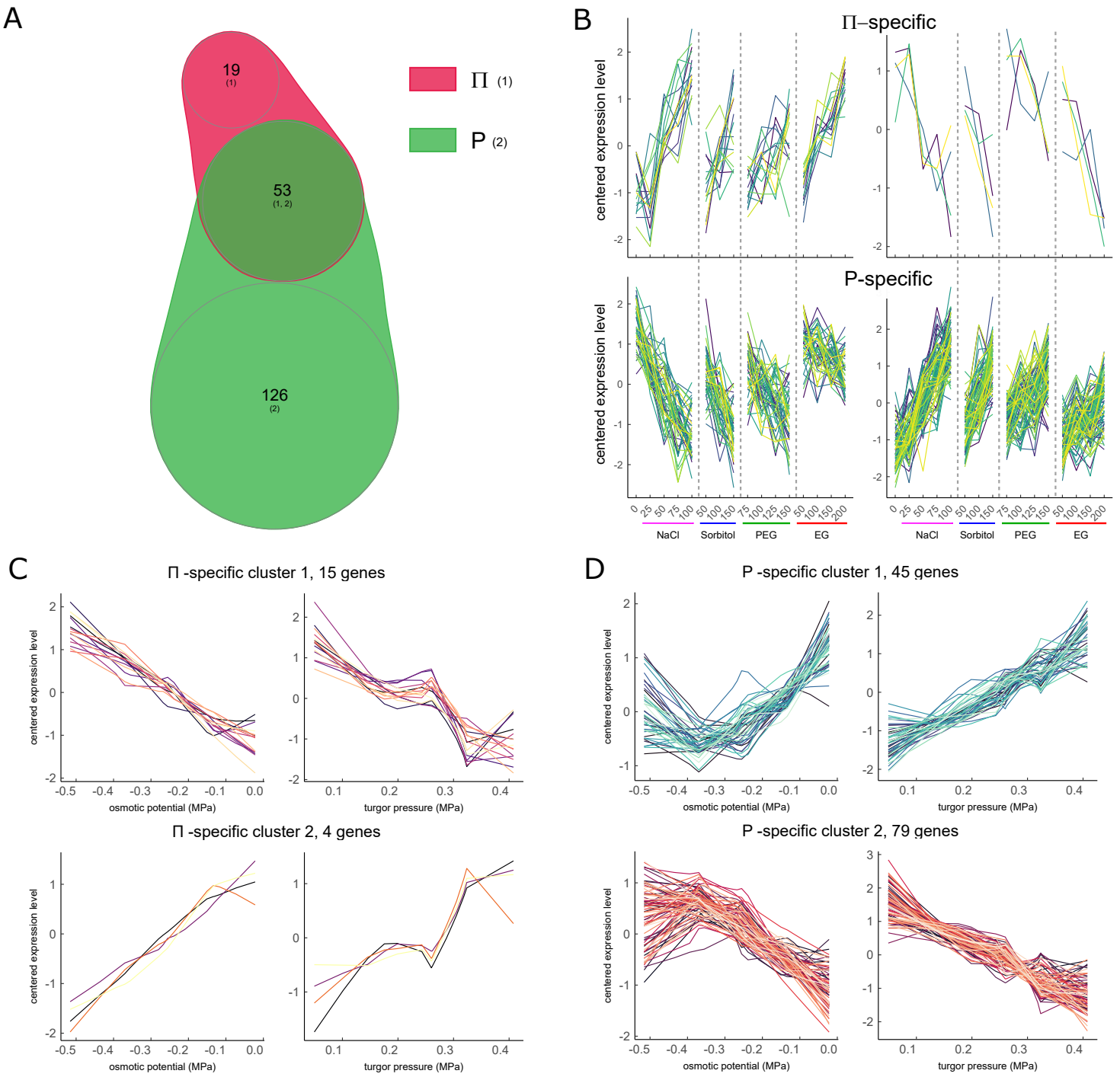

Figure 3

A: Venn diagram showing the number of genes, in the same transcriptomic approach as in figure 2, which expression is significantly correlated to Pi, P, or both. B: The 137 "Pi-specific" genes and 401 "P-specific" genes were split in 2 clusters each, and their average centered expression is expressed as a function of the solute/treatment combination corresponding to the biological assays of the transcriptome approach. C: The 137 "Pi-specific" genes were separated into 2 clusters and their average centered expression is expressed as a function of the osmotic potential of the solution of treatment, or the cortical cell turgor pressure. D: same representation as in C but for the 401 "P-specific" genes.

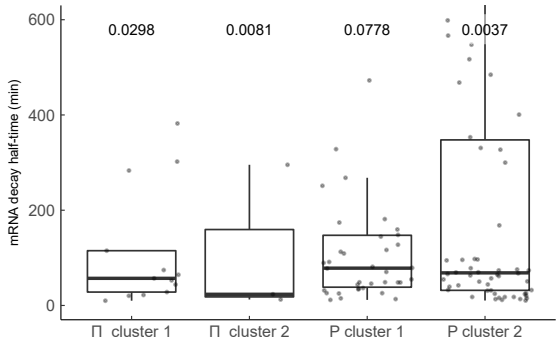

Figure 4

The half-life time of mRNAs (T1/2) was calculated from Sorenson et al. 2018, based on the decay rate ( ) modeled upon cordycepin treatment on sov mutant seedlings (i.e. Col 0, T1/2= ln(2)/) (Sorenson et al., 2018). T1/2 of each mRNA from genes in the clusters are presented individually and as boxplots. The numbers above the boxplots correspond the p-value of a bootstrap based test of T1/2 of the cluster being smaller than the whole genome median T1/2 (see M&M).

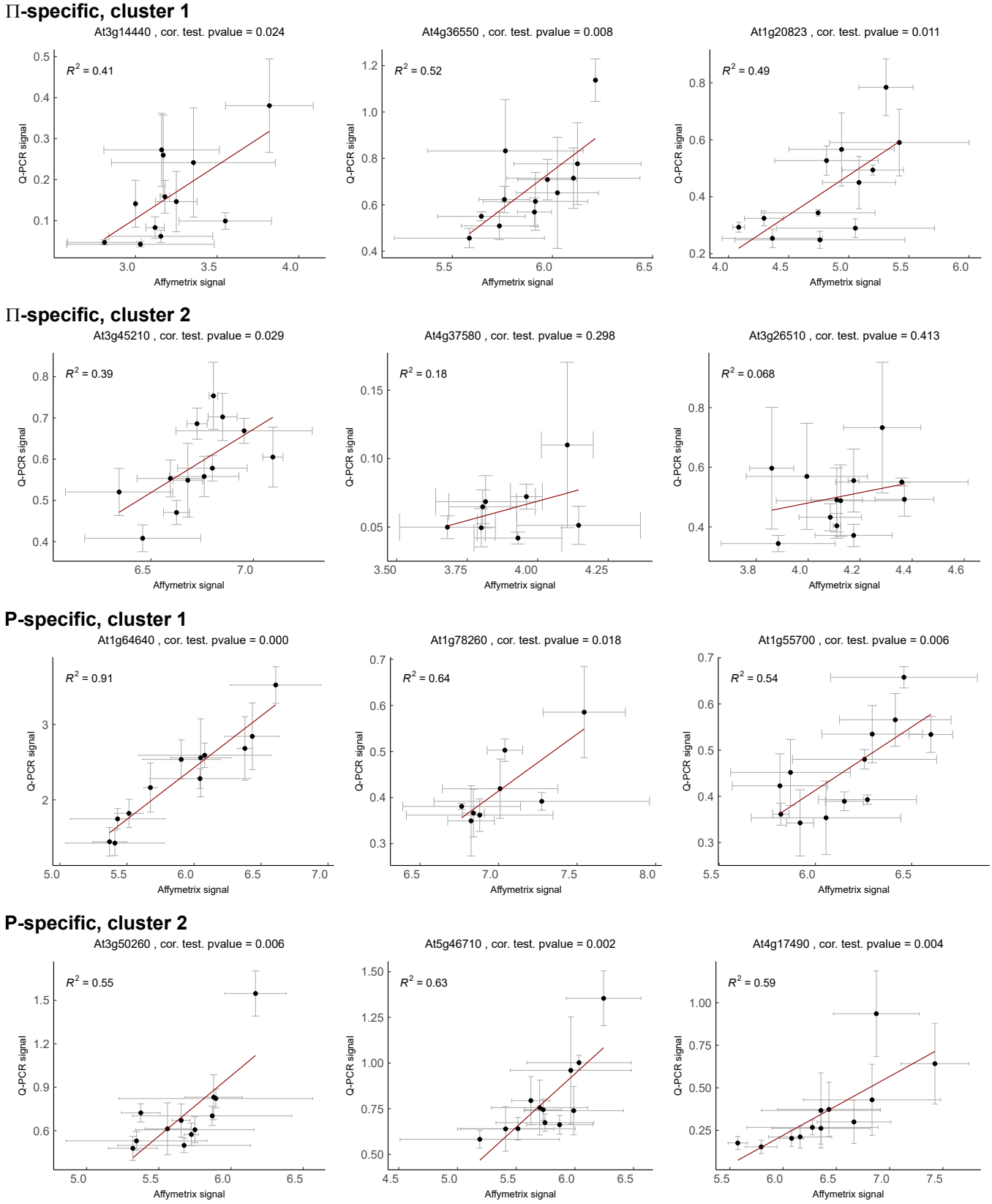

Figure 5

The expression of three candidates per list: or P, clusters 1 and 2 were investigated by RT-qPCR in 3 independent biological replicates. The plants were harvested 15min after transfer into a hydroponic solution, or the solution complemented with 25, 50,75, 100mM NaCl, or 50, 100, 150mM Sorbitol, or 50, 100, 150, 200g.l-1 EG. For each gene, normalized RT-qPCR signal (± SEM) is expressed as a function of the averaged signal (± SEM) obtained from the transcriptome analysis. The p-value of a correlation test (Pearson) as well as the linear fit (with its R² value) between the average values are indicated for each gene.

A

B

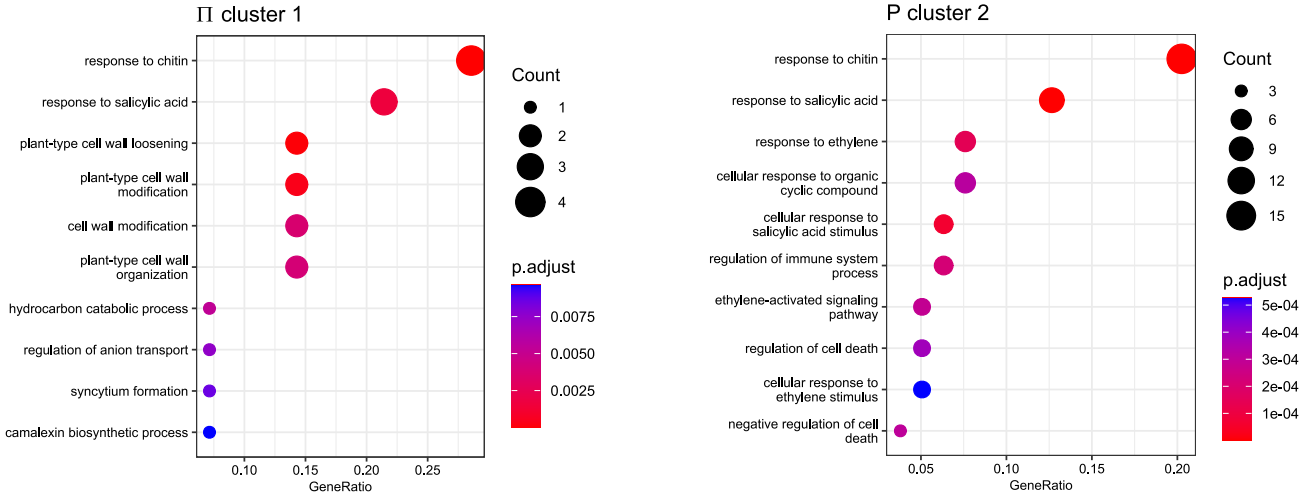

C

	GO response to stimulus	GO response to abiotic stimulus	GO response to salt stress	general stress response	transcription factor	Π-specific cluster 1	Π-specific cluster 2	P-specific cluster 1	P-specific cluster 2
GO response to stimulus		83.3	31.2	10	16.5	2.5		1.6	4.2
GO response to abiotic stimulus			59.2	14.6	17.6	3.1		0.8	4.2
GO response to salt stress				8.7	4.9	1.5			0.7
general stress response					5.2	9.7			7.7
transcription factor						2			3.3
Π-specific cluster 1							-0.4	-0.7	-0.9
Π-specific cluster 2								-0.5	-0.5
P-specific cluster 1									-1
P-specific cluster 2									

Figure 6

A: output of the Genecloud semantic analysis for the 2 clusters showing a significant enrichment. B: Output of a gene ontology analysis for the 2 clusters showing significant enrichments in GO terms. The GO terms, gene counts for each GO term and adjusted p-value of the enrichment are presented. C: Degree of overlap (Z-score) between our genes lists and public genes lists related to osmotic stress, the general stress response, and a list of transcription factors, using the Genesect algorithm.